Psychiatry Research 342 (2024) 116189

Contents lists available at ScienceDirect

Psychiatry Research

journal homepage: www.elsevier.com/locate/psychres

Abnormal inter-hemispheric effective connectivity from left to right auditory regions during Mismatch Negativity (MMN) tasks in psychosis

Christian Valt [a], Fran López-Caballero [b], Angelantonio Tavella [a,c], Mario Altamura [e], Antonello Bellomo [e], Giuseppe Barrasso [f], Brian Coffman [b], Filippo Iovine [f], Antonio Rampino [a,d], Alessandro Saponaro [g], Dylan Seebold [b], Pierluigi Selvaggi [a,d], Domenico Semisa [c], Giuseppe Stolfa [a], Alessandro Bertolino [a,d], Giulio Pergola [a,h,i,*,1], Dean F. Salisbury [b,1,**]

[a] Department of Translational Biomedicine and Neuroscience, University of Bari Aldo Moro, Bari, Italy
[b] Clinical Neurophysiology Research Laboratory, Western Psychiatric Hospital, University of Pittsburgh School of Medicine, Pittsburgh, PA, United States
[c] Department of Mental Health, ASL Bari, Bari, Italy
[d] Department of Psychiatry, Bari University Hospital, Bari, Italy
[e] Department of Clinical and Experimental Medicine, University of Foggia, Foggia, Italy
[f] Department of Mental Health, ASL Barletta-Andria-Trani, Andria, Italy
[g] Department of Mental Health, ASL Brindisi, Brindisi, Italy
[h] Lieber Institute for Brain Development, Johns Hopkins Medical Campus, Baltimore, MD, United States
[i] Department of Psychiatry and Behavioral Sciences, Johns Hopkins School of Medicine, Baltimore, MD, United States

ARTICLE INFO

Keywords:
Mismatch Negativity (MMN)
Granger causality
Psychosis
Inter-hemispheric connectivity deficit
Dysconnection hypothesis

ABSTRACT

Anomalous Mismatch Negativity (MMN) in psychosis could be a consequence of disturbed neural oscillatory activity at sensory/perceptual stages of stimulus processing. This study investigated effective connectivity within and between the auditory regions during auditory odd-ball deviance tasks. The analyses were performed on two magnetoencephalography (MEG) datasets: one on duration MMN in a cohort with various diagnoses within the psychosis spectrum and neurotypical controls, and one on duration and pitch MMN in first-episode psychosis patients and matched neurotypical controls. We applied spectral Granger causality to MEG source-reconstructed signals to compute effective connectivity within and between the left and right auditory regions. Both experiments showed that duration-deviance detection was associated with early increases of effective connectivity in the beta band followed by increases in the alpha and theta bands, with the connectivity strength linked to the laterality of the MMN amplitude. Compared to controls, people with psychosis had overall smaller effective connectivity, particularly from left to right auditory regions, in the pathway where bilateral information converges toward lateralized processing, often rightward. Blunted MMN in psychosis might reflect a deficit in inter-hemispheric communication between auditory regions, highlighting a "dysconnection" already at preattentive stages of stimulus processing as a model system of widespread pathophysiology.

1. Introduction

Friston's dysconnection hypothesis posits that schizophrenia results from disrupted functional connectivity of neural circuits, hindering effective communication between brain regions (Friston and Frith, 1995; Friston et al., 2016). Disturbed communication between brain regions in psychosis might be present already at the perceptual stages of stimulus processing. Auditory Mismatch Negativity (MMN), elicited in response to stimulus deviance from repetitive patterns, is blunted in schizophrenia (Näätänen and Kähkönen, 2009) and at psychosis onset (Salisbury et al., 2002; 2007). Its manifestation requires intact brain connectivity patterns (Lee et al., 2017). Hence, reduced auditory MMN

* Corresponding author at: Department of Translational Biomedicine and Neuroscience, University of Bari Aldo Moro, Piazza Giulio Cesare, 11, IT, Bari 70124, Italy.
** Corresponding author at: Clinical Neurophysiology Research Laboratory, Western Psychiatric Hospital, University of Pittsburgh School of Medicine, 3501 Forbes Ave, Suite 420, Pittsburgh, PA 15213, United States.
E-mail addresses: giulio.pergola@uniba.it (G. Pergola), salisburyd@upmc.edu (D.F. Salisbury).
[1] Equal contribution as senior authors.

https://doi.org/10.1016/j.psychres.2024.116189
Received 7 May 2024; Received in revised form 19 August 2024; Accepted 10 September 2024
Available online 11 September 2024

in psychosis might reflect abnormal functional connectivity linked to basic cell/circuit dysfunction.

MMN is an event-related potential (ERP) of brain activity that reflects the automatic detection of deviant stimuli in a sequence of standard stimuli (Näätänen et al., 2007). It is a negative deflection at approximately 150–250 ms post-stimulus in the waveform obtained by subtracting the ERP of standard stimuli from that of deviant stimuli (Näätänen et al., 2011). MMN is considered a prediction error signal for updating the predictive model of the sensory input (Friston, 2005; Lieder et al., 2013). Amplitude reductions have consistently been identified in schizophrenia (Tada et al., 2019) and other psychotic spectrum disorders (Erickson et al., 2016; Valt et al., 2023). Blunted MMN has also been observed in people at clinical high risk for schizophrenia (Aeberli et al., 2023): A group of individuals with early warning signs or subthreshold symptoms who have a 25 % chance of developing psychosis after two years (de Pablo et al., 2021). Recent studies with large cohorts dispute the presence of an MMN deficit in people at risk (Dheerendra et al., 2024), particularly for those who do not convert to full-blown psychosis (Hamilton et al., 2022). MMN is a promising biomarker of psychosis (Wang et al., 2022), useful for predicting psychosis in individuals at risk (Näätänen et al., 2016) and monitoring the course of the illness and the efficacy of interventions (Todd et al., 2023b). Even when MMN is not particularly reduced in early psychosis, it correlates with the gray matter volumes of MMN generators (Curtis et al., 2021; Salisbury et al., 2020), indicating its sensitivity to other aspects of auditory circuitry alterations proximal to psychosis onset.

Auditory MMN originates in the bilateral primary auditory cortex (A1) and the superior temporal gyrus (STG), and also likely includes contributions from the inferior frontal gyrus (IFG) (Garrido et al., 2009). At the spectral level, MMN is associated with increased power and phase synchronization in the theta band (Fuentemilla et al., 2008). Theta phase reset plays a crucial role in the brain's detection of deviant stimuli (Lakatos et al., 2020). Reductions of theta phase synchronizations are common observations in schizophrenia (Javitt et al., 2018; Valt et al., 2023), with the deficit extending to alpha activity (Sauer et al., 2023). Alpha and beta activities are thought to mediate the transfer of prediction signals between auditory areas (Chao et al., 2018). They show sensitivity to stimulus changes, while theta seems involved in feature integration for the comparison with the memory traces (Xia et al., 2023).

The connectivity within the temporo-frontal network for auditory deviance detection in schizophrenia has been principally investigated using dynamic causal modeling (DCM) (Braeutigam et al., 2018; Dima et al., 2012; Kirihara et al., 2020; Larsen et al., 2020; López-Caballero et al., 2024). DCM is a method that quantifies the effective connectivity between different brain regions by modeling the dynamic interactions and influences among them, with dipole-based source activity in each region modeled by a canonical microcircuit (David et al., 2006). DCM studies show low intrinsic effective connectivity in A1 in psychosis, with further modulations in forward and backward connections between STG and IFG (Dima et al., 2012; Todd et al., 2023a). Integrating inter-hemispheric connections in the DCM model, patients with a psychiatric disorder show low connectivity from the left to the right STG, but this deficit seems to be stronger for non-psychotic than psychotic patients (Larsen et al., 2020).

Granger causality is an alternative method for the study of brain connectivity. Unlike DCM, which creates complex circuit models to explain observed data, Granger causality reconstructs effective connectivity based on the information flow between two brain regions using essentially model independent time-series of activity (Friston et al., 2013). Two studies investigated Granger causality in schizophrenia during an MMN task. Koshiyama et al. (2020) reported that patients with schizophrenia showed increased spectral (2–14 Hz) connectivity from ipsilateral mid-temporal and contralateral cingulate and calcarine areas to the right prefrontal cortex, in conjunction with decreased inter-hemispheric connectivity from left pre-central areas to the right mid-frontal and frontal inferior operculum regions. Yüksel et al. (2021) found diminished right to left inter-hemispheric connectivity for broadband ERP activity in patients with a first episode of psychosis. However, both experiments down-sampled the data, reducing the sensitivity of Granger causality for fast influences. Moreover, although the first study used sliding windows to track changes in Granger causality over time, the second study used only one 350 ms long window. Since network reconfigurations associated with MMN are brief (Nicol et al., 2012), investigating fast causal effects might provide better insight into network dynamics, getting closer to brain processing speed.

This study investigated the nature of the connectivity deficit in psychosis during an MMN task, examining the relevance of left-to-right connectivity. Granger causality in response to standard and deviant stimuli was analyzed with sliding time windows, looking for causal effects in a lag of 10 time points that corresponded to activity occurring within 10 ms before the time point of interest. Analyses were conducted on two different magnetoencephalography (MEG) datasets, one collected by the Group of Psychiatric Neuroscience of the University of Bari Aldo Moro (Italy) and the other by the Clinical Neurophysiology Research Laboratory of the University of Pittsburgh (PA, USA). Having two datasets allows for comparing the method's accuracy and assessing the reliability and generalizability of the clinical findings.

Compared to previous investigations of Granger causality that used EEG, reconstructing MEG signals into brain sources mapped on individual structural MRI (sMRI) allows a precise investigation of the brain networks of interest. MEG sensitivity to radial activity makes this method ideal for studying the bilateral auditory areas, with the limit that frontal activity associated with magnetic MMN (MMNm) is mostly undetectable. Hence, this study focused on effective connectivity within and between the auditory regions. We investigated theta, alpha, and beta frequency ranges since they reflect different processing stages in deviance detection (Xia et al., 2023).

Besides overall diminished effective connectivity within and between auditory regions in psychosis, based on Larson et al.'s (2020) and Koshiyama et al.'s (2020) findings, we specifically expected significant abnormalities in left-to-right inter-hemispheric connectivity. Hypothesizing that the reported discrepancies in intrinsic connectivity in the right and left auditory regions in schizophrenia (Dima et al., 2012; Todd et al., 2023a) might reflect MMNm lateralization variability, we expected an association between the strength of effective connectivity within and from an auditory region with MMNm laterality. Stronger effective connectivity within and from the left auditory region should be evident when the MMNm amplitude is larger in the left than in the right hemisphere. Moreover, we explored the relationship between effective connectivity and the MMNm source-reconstructed amplitudes in the left and right auditory regions.

Experiment 1 (Bari)

2. Methods

2.1. Participants

From a comprehensive cohort of 432 people tested at the University of Bari Aldo Moro, 228 participants had MEG and sMRI recordings. Within this subset, 147 participants were healthy people with no history of neurological or psychiatric disorders (Neurotypical Controls, NC; mean age: 27 years, range: 17–59; M/F: 66/81). The remaining 81 participants were people with a diagnosis that fell within the psychotic spectrum (People with or at risk for Psychosis, PP; mean age: 27 years, range: 15–65; M/F: 49/32). All PP and nearly half of NC were tested in a previous study on MMNm deficit in psychosis (Valt et al., 2023).

PP were recruited from the outpatient and inpatient services of the Psychiatric Clinic of the University Hospital of Bari. According to the Structured Clinical Interview for DSM-V, 26 had a diagnosis of schizophrenia or schizoaffective disorder, 16 had a diagnosis of Type-I bipolar disorder with psychotic symptoms, 10 had experienced a first psychotic episode within the previous twelve months, while 29 were classified as

clinical-high risk on the Italian version of the Comprehensive Assessment of At-Risk Mental States (CAARMS; Yung et al., 2005). In cases where pharmacological intervention was recommended, PP were tested after one month of stable treatment.

The Ethics Committee of the University Hospital of Bari approved this study. Eligible participants were informed verbally and with an information sheet about the purposes of the MEG/MRI experiment and signed written consent statements.

2.2. MMN task

Participants performed a passive auditory odd-ball task with duration deviant stimuli (Michie et al., 2000). In this paradigm, a sequence of pure tones (1000 Hz, 80 dB) was presented to both ears while participants watched a silent Tom & Jerry cartoon. The tone sequence consisted of 612 50-ms-long standard stimuli, sporadically interrupted by 55 100-ms-long deviant stimuli. The inter-stimulus interval was set to 500 ms.

2.3. MRI data acquisition and processing

Each participant underwent a T1-weighted sMRI using a Philips Ingenia 3T scanner with a T1-FFE sequence ($1 \times 1 \times 1$ mm^3 resolution, 180 slices, TR and TE: shortest, FOV: 256 mm). Offline, sMRI images were segmented into white matter, gray matter, and cerebrospinal fluid using the Computational Anatomy Toolbox 12 (CAT12; Gaser, et al., 2024). In Brainstorm (Tadel et al., 2011), we derived individual head models from the T1-weighted sMRI, downsampled to 15,002 vertices, and estimates of left and right cortical surfaces and thickness. For coregistration purposes, six landmarks were manually identified on the individual sMRI (anterior and posterior commissures, nasion, bilateral preauricular points, and interhemispheric fissure). Finally, a visual inspection ensured the procedural accuracy and the absence of morphological alterations.

2.4. MEG data acquisition and processing

The MEG signal was recorded in a magnetically shielded room using a 306-channel Elekta Neuromag® TRIUX whole-head system (Elekta Neuromag Oy, Helsinki, Finland). Before the recording, we marked three fiducial points (nasion, left and right periauricular points) for the coregistration of sMRI and MEG data, along with one hundred additional points covering the scalp for head reconstruction. The participant's head position relative to the MEG sensors was continuously monitored using a 3D digitizer (ISOTRAK; Polhemus, Inc., Colchester, VT), tracking the positions of five head position indicator coils placed on the participant's head (two on the left and right mastoids and three on the forehead). Data were recorded at a sampling rate of 1000 Hz with an online band-pass filter from 0.1 to 330 Hz.

Offline, the signal underwent initial processing using Elekta MaxFilter™ software (Elekta Neuromag Oy, Helsinki, Finland) for noise removal around the MEG helmet with temporal Signal-Space Separation (tSSS) (Taulu and Simola, 2006) and head movement correction. Subsequently, we applied the standard group analysis processing pipeline for Brainstorm (Tadel et al., 2011), as outlined by Tadel et al. (2019). This pipeline involved filtering the signal to eliminate the standard European electricity grid frequency (notch filter: 50 Hz) and high-frequency artifacts (low-pass filter: 60 Hz). We then identified and corrected eye movements and heartbeat artifacts based on Independent Component Analysis (runica function with 20 components). The remaining artifacts were automatically detected and rejected (reference activity 0–60 s, 1 s time windows; conservative detection with a sensitivity parameter of 5).

Epochs were subsequently segmented from 200 ms before to 500 ms after stimulus onset. The analysis considered only artifact-free deviant and a subset of artifact-free standard stimuli, i.e., those preceding each deviant stimulus, to obtain an equal number of standard and deviant stimuli.

2.5. MEG source localization

MEG sensors and the individual structural brain image were coregistered by aligning the three fiducial points with the correspondent points in the sMRI image, manually adjusted according to the reconstructed head shape when needed. The forward solution was modeled as overlapping spheres with 15,002 vertices. MEG activity was projected to dipoles at each vertex with Minimum Norm Imaging estimation (Baillet et al., 2001). Source activity was computed with dSPM (Dale et al., 2000) in constrained dipole orientations regularized based on a noise covariance matrix derived from a 2 min empty-room recording (depth weighting with an order of 0.5 and a maximal amount set at 10; regularization of 0.1; signal-to-noise ratio of 3.0).

2.6. Granger causality computation

We performed bivariate spectral Granger causality across vertices corresponding to the right and left transverse temporal sulcus, superior temporal gyrus, and transverse temporal gyrus of the Destrieux atlas (Destrieux et al., 2010). The analysis was performed on concatenated 100 ms long segments of artifact-free trials, with the time window moving in 10 ms steps starting with the segment −100:0 and ending with the segment 300:400. The Granger causality analysis considered ten equally spaced frequencies, ranging from 2 to 20 Hz with an order of 10. Granger values were averaged for bivariate contrasts of vertices within the left (from left to left: Ll), the right (from right to right: Rr), and between the auditory regions (from left to right and from right to left: Lr and Rl, respectively).

The subtraction of Granger values for standard stimuli from Granger values for deviant stimuli resulted in an index of effective connectivity for deviance detection. We analyzed theta (4–8 Hz), alpha (10–12 Hz), and beta (14–20 Hz) activities separately because they reflect different processes in deviance detection (Xia et al., 2023). Effective connectivity was estimated as the maximum Granger value in time windows ranging from 0:100 to 250:350.

2.7. MMNm event-related field (ERF) computation

In the ERF analysis, the mean source-based signals for standard and deviant stimuli were transformed into absolute values before averaging across vertices of the left and right auditory regions. The MMNm ERF peak amplitude was determined as the maximum amplitude between 150 and 225 ms in the signal resulting from the subtraction of the standard from the deviant ERFs.

2.8. Analysis

Preliminarily, the MEG data were analyzed as ERF to assess whether people at risk for psychosis and patients with psychosis presented significantly different MMNm amplitudes.

Granger values were analyzed with ANOVAs examining the within-participant factors Laterality (left and right) and Connectivity (intra-region and inter-hemisphere) and the between-participants factor Group (PP vs. NC). Since MMNm amplitude correlates significantly with age (Valt et al., 2023), the participant's age was used as a covariate.

Permutation tests were performed 10,000 times independently for each connectivity direction. This permutation procedure was performed 100 times by randomly selecting 82 NC to account for the difference in sample size between NC and PP. The p-value was derived as the proportion of permuted test statistics equal to or greater than the p-value of the unshuffled groups. The final p-value was the mean p-value across all iterations.

The relationship between beta, alpha, and theta effective

connectivity in the four directions and MMNm peak amplitude was examined by linear regressions using stepwise modeling. This test was also used to investigate whether the laterality and direction of Granger causality were related to MMNm laterality. To this end, we computed Granger causality and MMNm laterality indexes by subtracting the values computed in the right auditory regions from those in the left.

3. Result

Data from two NC were excluded from all the analyses because they presented Granger values and MMNm peak amplitudes overshooting 1.5-fold the interquartile range of the sample (see supplementary material).

In the preliminary ERF analysis, Group was significant, $F(2,222) = 11.17$, $p < .001$, $\eta_p^2 = .091$. MMNm peak amplitudes were significantly greater in NC than in patients with psychosis, $t = 4.23$, $p_{holm} < .001$, or those at risk, $t = 2.73$, $p_{holm} = .014$, without significant differences between the two clinical populations, $t = 0.48$, $p_{holm} = .635$ (see Fig. 1). Hence, we combined these two populations into a single group for subsequent Granger causality analyses (see Fig. 2) (see the supplementary material for the analyses that considered the four clinical subgroups separately (CHR, FEP, BD, and SCZ) or CHR alone).

3.1. Granger causality

Although Granger values showed significant correlations across the three frequency bands ($rs > 0.69$, $ps < .001$), the latency of the maximal effective connectivity in the three frequency bands differed significantly, $F(2,450) = 3.25$, $p = .040$, $\eta_p^2 = .01$. Specifically, the peak of beta effective connectivity occurred earlier than the peak of theta effective connectivity, $t = 2.50$, $p_{Holm} = .038$ (see, Fig. 3), while the latency of alpha effective connectivity was intermediate between the other two but did not differ significantly, $ts < 1.67$, $ps_{Holm} > .192$.

In the beta band (see Fig. 3, blue waves), there was a significant effect of Laterality, $F(1,223) = 4.45$, $p = .036$ $\eta_p^2 = .020$, but no significant effect of Connectivity, $F(1,223) = 0.02$, $p = .895$, or Laterality by Connectivity interaction, $F(1,223) = 0.30$, $p = .583$. The right auditory region showed stronger effective connectivity than the left, both within

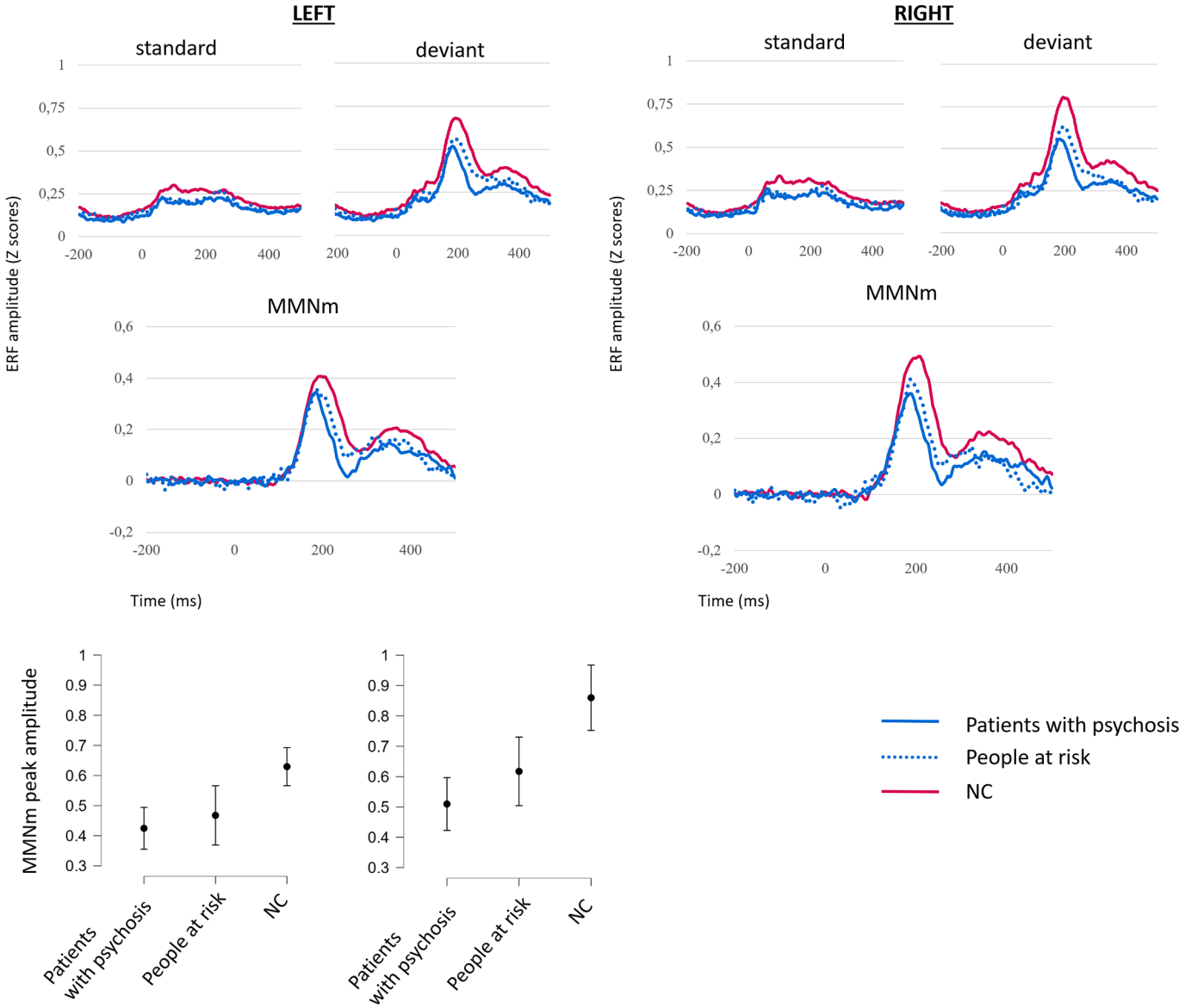

Fig. 1. Line plots: ERF waveforms for standard, deviant, and MMNm (deviant-standard) in the Neurotypical Controls (NC), people at risk, and patients with psychosis, separately displaying activity in the left and the right auditory region. Interval plots: mean with 95 % confidence interval for the MMNm peak amplitudes in the three groups.

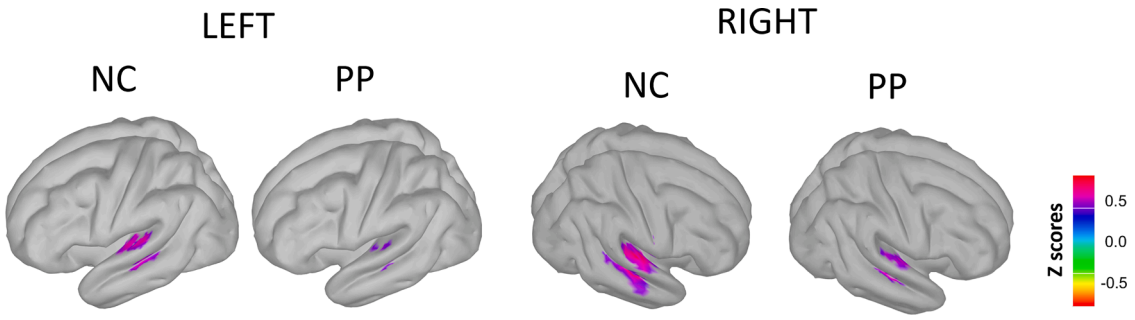

Fig. 2. Brain maps: MMNm source reconstructed activity in the right and the left hemisphere for Neurotypical Controls (NC) and People with or at risk for Psychosis (PP) in the Bari sample.

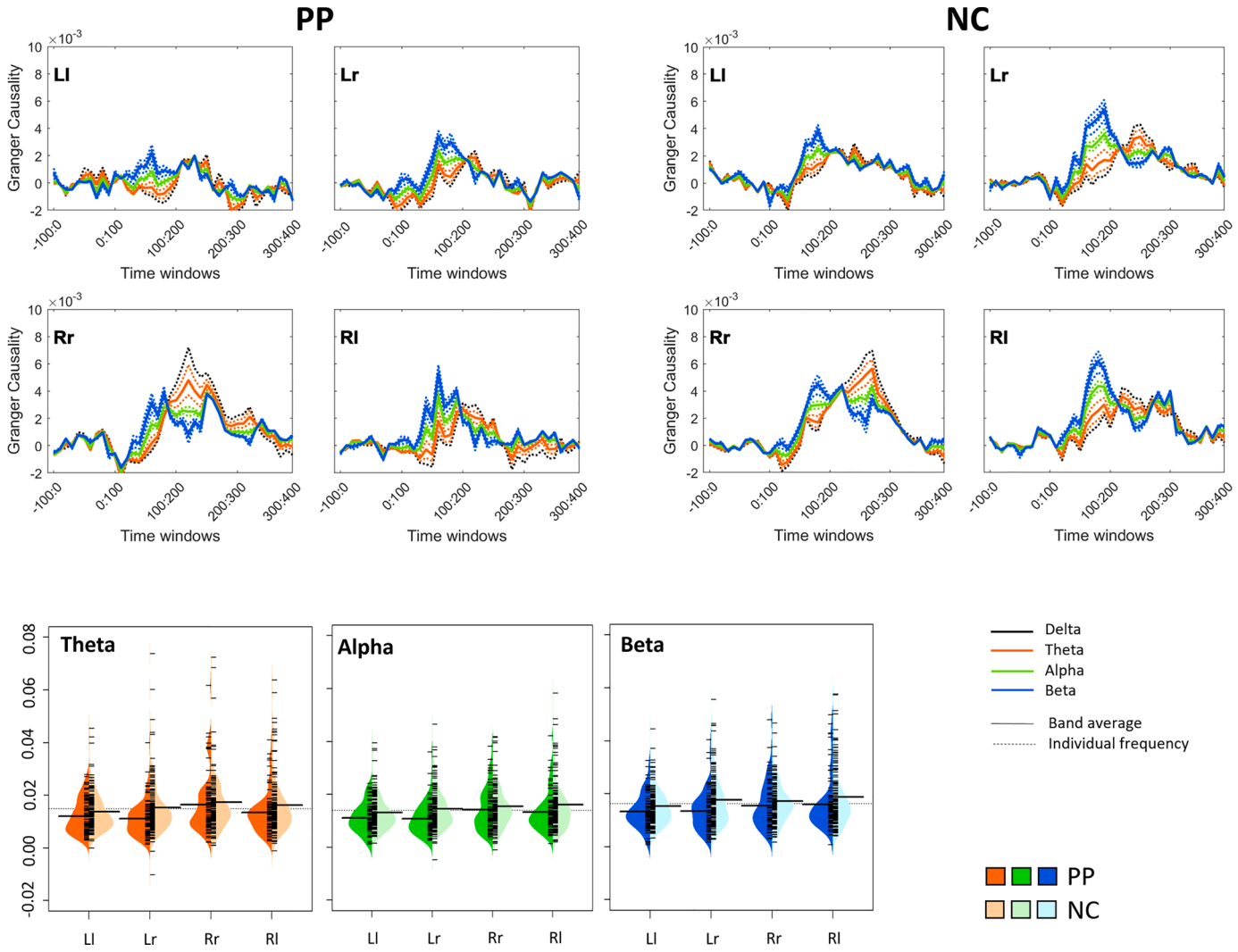

Fig. 3. Line plots: MMNm Granger causality (deviant minus standard) over time windows, displayed separately for People with or at risk for Psychosis (PP) and Neurotypical Controls (NC) in the four connectivity directions: left-to-left (Ll), left-to-right (Lr), right-to-right (Rr), and right-to-left (Rl). Beanplot: Distribution of the maximum Granger causality values between the time windows 0:100 and 250:350. Each beanplot displays within the same figure the data distribution for PP on the left (dark colors) and for NC on the right (light colors). The two large black lines reflect the two group means, while the small lines reflect the individual observations.

and across hemispheres. Group was only significant as a main effect, $F(1,223) = 9.31$, $p = .003$, $\eta_p^2 = .040$ (all interactions, $Fs(1,223) < 2.11$, $ps > 0.148$): PP showed weaker beta-band effective connectivity within and between auditory regions than NC.

In the alpha band (see Fig. 3, green waves), the pattern of significant results was similar to that of beta-band effective connectivity, with significant effects of Laterality, $F(1,223) = 6.90$, $p = .009$, $\eta_p^2 = .030$, and Group, $F(1,223) = 10.67$, $p = .001$, $\eta_p^2 = .046$ (all other effects or interactions, $Fs(1,223) < 2.58$, $ps > .110$).

In the theta band (see Fig. 3, orange waves), besides the significant effects of Laterality, $F(1,223) = 4.48$, $p = .035$, $\eta_p^2 = .020$, and Group, $F(1,223) = 7.73$, $p = .006$, $\eta_p^2 = .034$, there was also a trend toward significance in the interaction between Connectivity and Group, $F(1,223) = 3.06$, $p = .082$ (all other effects or interactions, $Fs(1,223) < 0.42$, $ps >$

.518).

Permutation analyses showed that PP and NC differed significantly in left-to-right inter-hemispheric connectivity both for beta, $p = .002$, alpha, $p < .001$, and theta frequencies, $p = .002$, and in alpha right-to-left inter-hemispheric connectivity, $p = .035$ (all other tests: $ps > .051$).

3.2. Granger causality and MMNm amplitude

A model with beta ($t = 5.39$, $p < .001$) and theta ($t = 2.70$, $p = .008$) left-to-right inter-hemispheric and beta left intra-region ($t = 3.21$, $p = .002$) effective connectivity was the best predictor of the variance in left MMNm ERF amplitude, $F(3,222) = 36.90$, $p < .001$ (Adjusted $R^2 = 0.32$). On the other hand, a model with theta right-to-left ($t = 2.37$, $p = .019$) and left-to-right ($t = 2.25$, $p = .026$) inter-hemispheric and alpha right intra-region ($t = 4.43$, $p < .001$) effective connectivity explained a significant amount of the variance in the right MMNm ERF amplitude $F(3,222) = 15.64$, $p < .001$ (Adjusted $R^2 = 0.16$).

The beta ($t = 3.24$, $p = .001$) and alpha ($t = 3.19$, $p = .002$) inter-hemispheric Granger causality left-right difference significantly explained the MMNm ERF amplitude left-right difference, $F(2,223) = 12.84$, $p < .001$ (Adjusted $R^2 = 0.10$).

Experiment 2 (Pittsburgh)

4. Method

4.1. Participants

This sample is an extended group of the participants analyzed by López-Caballero et al. (2023): 36 NC (mean age: 24 years, range: 18–39; M/F: 23/13) and 37 first-episode psychosis patients (FEP (mean age: 22 years, range: 15–34; M/F: 27/10). FEP were recruited from the outpatient and inpatient services of the University of Pittsburgh Medical Center Western Psychiatry Hospital. Based on the Structured Clinical Interview for DSM-IV (First et al., 2014) performed by expert clinicians, FEP participants had a diagnosis of schizophrenia (undifferentiated, $N = 9$; residual, $N = 1$; paranoid: $N = 9$), schizoaffective disorder ($N = 1$), schizophreniform disorder ($N = 3$), psychotic disorder not otherwise specified ($N = 6$), bipolar disorder with psychotic features ($N = 5$) and major depressive disorder with psychotic features ($N = 3$). They underwent testing within one year of their initial clinical contact for psychosis, all with less than one year of lifetime pharmacological treatment. All participants had normal hearing as assessed by audiometry (within 30 dB nHL and <15 dB difference between ears from 500 to 4000 Hz).

The Institutional Review Board of the University of Pittsburgh approved this study. All participants gave written informed consent and received compensation for participating in the experiment.

4.2. MMN task

Participants performed a passive auditory odd-ball task with duration and pitch deviant stimuli. A sequence of 1200 standard tones (frequency: 1000 Hz; duration: 50 ms) was randomly interrupted by 150 pitch deviant tones (frequency: 1200 Hz; duration: 50 ms) and 150 duration deviant tones (frequency: 1000 Hz; duration: 100 ms). The stimulus onset asynchrony was set to 330 ms.

4.3. Data processing and acquisition

The parameters described above for the Bari dataset were consistently applied here to offline MEG data processing, MEG source localization, Granger causality estimation, and MMNm ERF computations (see supplementary material for details on MRI and MEG data acquisition and processing).

4.4. Analysis

This study focused on duration deviant stimuli (Figs. 4 and 5) since FEP and NC did not differ significantly in MMNm amplitudes for pitch deviant stimuli (see López-Caballero et al. 2023). The statistical analyses were identical to the ones outlined before, except for permutation tests that always used the same NC (refer to the supplementary material for the results on effective connectivity in response to pitch deviant stimuli).

5. Results

5.1. Granger causality

Although Granger values showed significant correlations across the three frequency bands ($rs > 0.81$, $ps < .001$), the latency of the maximal effective connectivity in the three frequency bands differed significantly, $F(2,144) = 3.53$, $p = .032$, $\eta_p^2 = .050$. Specifically, the peak of beta effective connectivity occurred earlier than the peak of theta effective connectivity, $t = 2.57$, $p_{Holm} = .034$ (see Fig. 6), while the latency of alpha effective connectivity was intermediate between the other two but did not differ significantly, $ts < 1.88$, $ps_{Holm} > .124$.

In the beta and the alpha bands, no effect or interaction was significant: in beta, $Fs(1,70) < 2.71$, $ps > .105$, and in alpha, $Fs(1,70) < 2.60$, $ps > .111$ (see Fig. 6, blue and green waves).

In the theta band, there was a significant interaction between Group and Connectivity, $F(1,70) = 6.32$, $p = .014$, $\eta_p^2 = .08$ (all other effects or interactions, $Fs(1,70) < 2.48$, $ps > .120$). Compared to NC, FEP showed significantly smaller inter-hemispheric connectivity, $F(1,70) = 6.24$, $p = .015$, $\eta_p^2 = .082$, but no difference in intra-region connectivity, $F(1,70) = 0.01$, $p = .997$ (see Fig. 6, orange waves).

Permutation analyses showed smaller left-to-right inter-hemispheric connectivity in FEP than NC in theta, $p = .012$, alpha, $p = .032$, and beta, $p = .081$ (all other tests: $ps > .089$).

5.2. Granger causality and MMNm amplitude

A model with beta left intra-region ($t = 7.13$, $p < .001$) and theta right-to-left inter-hemispheric ($t = 4.17$, $p < .001$) effective connectivity explained a significant amount of the variance in left MMNm amplitude, $F(2,70) = 36.02$, $p < .001$ (Adjusted $R^2 = 0.49$), while a significant amount of the variance in right MMNm amplitude was explained by a model with beta left-to-right ($t = 2.98$, $p = .004$) and alpha right-to-left ($t = 2.35$, $p = .021$) inter-hemispheric effective connectivity, $F(2,70) = 17.27$, $p < .001$ (Adjusted $R^2 = 0.31$).

The alpha inter-hemispheric ($t = 3.40$, $p = .001$) Granger causality left-right difference significantly explained the MMNm ERF amplitude left-right difference, $F(1,71) = 11.52$, $p = .001$ (Adjusted $R^2 = 0.13$).

6. Discussion

The present study investigated effective connectivity associated with deviance detection in auditory MMN tasks, focusing on potential deficits in psychosis. We analyzed two MEG datasets with Granger causality within and between the bilateral auditory areas (correspondent to the transverse and the superior temporal gyri) in the theta-, alpha-, and beta-frequency bands. Deviance detection was associated with initial beta and subsequent alpha and theta increases in effective connectivity, with the direction of alpha effective connectivity correlating with MMNm laterality. That is, the hemisphere with greater directional influence showed a larger MMNm peak amplitude. Effective connectivity was reduced in patients, particularly for theta connectivity from the left to the right auditory regions. Importantly, patterns of effective connectivity deficit in psychosis were similar in the two datasets, indicating independent validation of findings.

Increases of effective connectivity within auditory sensory/perceptual cortices and between hemispheres during deviance detection

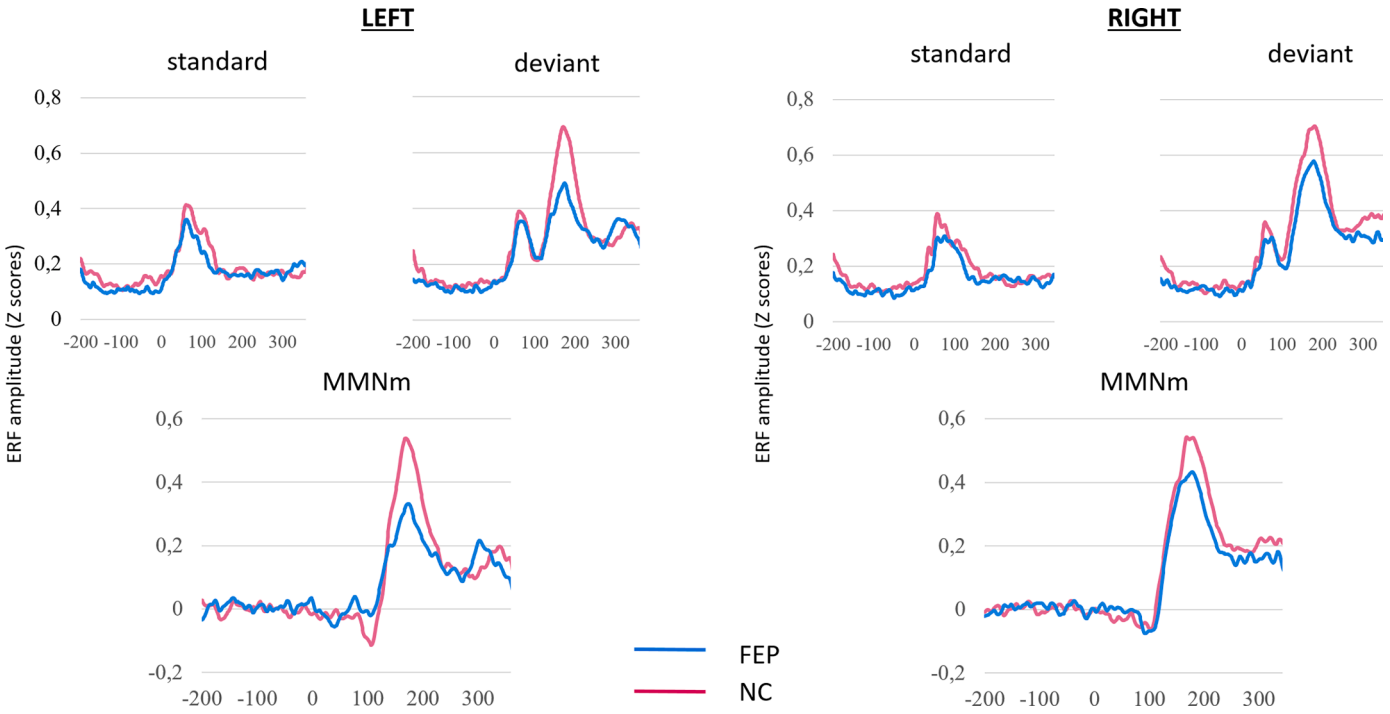

Fig. 4. Line plots: ERF waveforms for standard, deviant, and MMNm (deviant-standard) in Neurotypical Controls (NC) and First-Episode Psychosis (FEP).

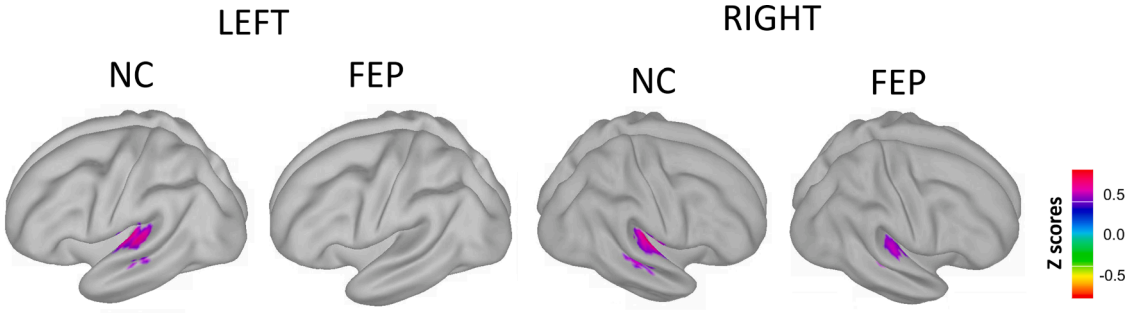

Fig. 5. Brain maps: MMNm source reconstructed activity in the right and the left hemisphere for Neurotypical Controls (NC) and First-Episode Psychosis (FEP) in the Pittsburgh sample.

occurred for both beta, alpha, and theta frequencies. Effective connectivity in beta and theta frequency bands reflects distinct yet closely related stages of deviance detection, as they are strongly correlated but temporally distinct: heightened effective connectivity in beta corresponds to later stronger effective connectivity in theta. Despite the lack of a latency effect, alpha connectivity was strongly correlated with both beta and theta connectivity. Beta and alpha activities are often not evident in time-frequency power and inter-trial phase coherence analyses, where theta activity is predominant instead (see Valt et al., 2023). Here, adopting a 10-ms interval for the Granger estimation, equivalent to 1/20 of a complete 5Hz-theta cycle, may have introduced a methodological limitation, leading to the underestimation of theta connectivity in favor of beta and alpha connectivity. Beta activations in deviance detection have been registered in intracranial recording in primates during a tone omission task (Suda et al., 2022) and *in vitro* models (Haenschel et al., 2000). Xia et al. (2023) described beta/alpha modulations for auditory stimuli with midpoint frequency changes and interpreted them as indicators of perceptual feature processing before integration into a unified representation in theta. Hence, beta and alpha effective connectivity might reflect the perceptual processing of the stimulus for the later generation of a prediction error, with theta linked to deviance from prior stimuli and higher-order predictive sensory models.

Theta frequencies showed the most consistent abnormalities across both experiments, particularly in inter-hemispheric left-to-right connectivity. Theta reductions in psychosis are common observations in spectral power and phase coherence (Javitt et al., 2018; Sauer et al., 2023; Valt et al., 2023; but, see also Dheerendra et al., 2024). Theta frequencies function as a means for communication between the localized processing of auditory stimuli in primary sensory areas and the broader network that involves hippocampal and frontal areas for generating prediction error signals (Recasens et al., 2018). Reduced theta effective connectivity might reflect impaired interplay between cortical pyramidal neurons and local circuit SST-type GABAergic interneurons (Javitt et al., 2018), affecting efficient perceptual processing and disrupting communication within higher-level brain networks. While our present experiment focused on connectivity within and between auditory regions, the reduced effective connectivity from left central to right frontal regions in psychosis reported by Koshiyama et al. (2020) allows for reasonable speculation that abnormal theta activity may reflect a deficit in the broader network responsible for prediction error estimation.

The observation of reduced effective connectivity in patients aligns with previous connectivity studies of MMN in psychosis (Braeutigam

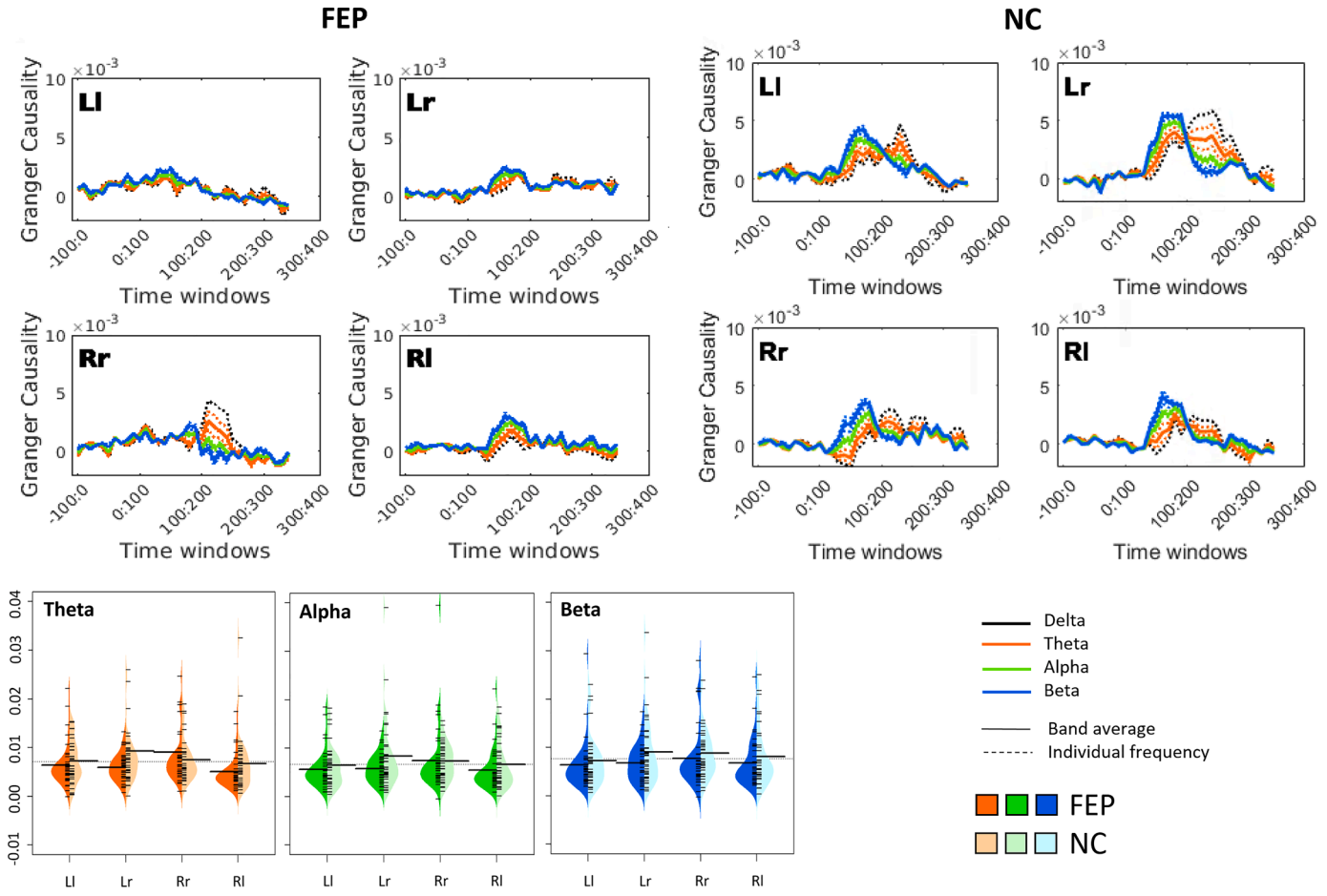

Fig. 6. Line plots: MMNm Granger causality (deviant minus standard) over time windows, displayed separately for First-Episode Psychosis patients (FEP) and Neurotypical Controls (NC) in the four connectivity directions: left-to-left (Ll), left-to-right (Lr), right-to-right (Rr), and right-to-left (Rl). Beanplot: Distribution of the maximum Granger causality values between the time windows 0:100 and 250:350. Each beanplot displays within the same figure the data distribution for FEP on the left (dark colors) and for NC on the right (light colors). The two large black lines reflect the two group means, while the small lines reflect the individual observations.

et al., 2018; Dima et al., 2012; Koshiyama et al., 2020; Larsen et al., 2020; Todd et al., 2023a; Yüksel et al., 2021). Hence, the MMN deficit in psychosis is not a mere reduction of brain activation but, rather, is, at least in part, the result of abnormalities in the coordinated communication between brain regions. The concurrent observation that the inter-hemispheric communication from left to right auditory regions shows the strongest deficit is consistent with a similar finding in the only DCM study that considered inter-hemispheric connectivity (Larsen et al., 2020; see also Koshiyama et al., 2020). In her influential MMN model, Garrido et al. (2007) hypothesized lateralization of late stages of deviance detection to the right frontal lobe. This model was later integrated with inter-hemispheric connections between temporal regions (Garrido et al., 2009; see also Schofield et al., 2009). According to Garrido et al.'s (2009) model, it is plausible to posit an information flow from the left to the right hemisphere, given the rightward lateralization of subsequent processes. However, inter-individual differences in the MMNm laterality and the concurrent difference in the direction of alpha inter-hemispheric connectivity suggest that, in a group of subjects, deviance detection might be lateralized to the left.

This is the first study of effective connectivity in psychosis to use a replication sample. Having found similar patterns of Granger causality and concordant group effects in two different MEG datasets indicates that the Granger analysis was adequate for detecting rapid causal communication within and between auditory regions and that the observed clinical results are reliable and generalizable across patient populations, tasks, recording procedures, and MEG scanners. However, the requirement to select a time window and concatenating trials might have reduced the estimation of Granger causality and the temporal precision of the analysis, particularly for low frequencies. These are two limits that the employment of sliding windows might have mitigated but not entirely resolved. Moreover, the limited sensitivity of MEG to MMN-related frontal activity imposed a focus on the bilateral temporal auditory regions, missing communication with frontal areas.

The impact of drugs on the observed outcomes was not assessed, but MMN alterations are not strictly linked to the use of psychotropic medications (Kool et al., 2022), with amplitude reductions also in drug-naïve patients (Li et al., 2023). Here, in Experiment 1, alterations of effective causality were observed also in people at risk: a population of young drug-naïve individuals with subclinical psychosis symptoms (see supplementary material). Importantly, given that over 80 % of individuals at clinical high risk for psychosis do not progress to develop clinically significant psychotic symptoms (de Pablo et al., 2021), the presence of blunted MMN in this group suggests that the observed deficit may be associated with broader psychopathological features rather than psychosis alone. MMN reductions are also present in depression (Tseng et al., 2021), but the deficit seems to be weaker than the one reported in psychosis (Kim et al., 2020; Kool et al., 2022; Umbricht et al., 2003). Hence, without patients outside the psychosis spectrum, we cannot establish that the reported effective connectivity deficit is a specific attribute of psychosis.

In conclusion, while beta, alpha, and theta frequencies exhibited significant group differences, theta frequencies, particularly in inter-hemispheric left-to-right connectivity, consistently showed abnormalities in psychosis, suggesting a deficit in the broader network responsible

for prediction error estimation in auditory processing. Reduced alpha and theta inter-hemispheric communication from left to right auditory areas imply that this “dysconnectivity” may represent a key MMN anomaly in psychosis, holding significant implications for network models of deviance detection in healthy and clinical populations.

Financial support

Work supported by #NEXTGENERATIONEU (NGEU) and funded by the Ministry of University and Research (MUR), National Recovery and Resilience Plan (NRRP), for the project PRISM (SOE_0000127) "Profiling the risk for schizophrenia with machine learning" to CV and the project MNESYS (PE0000006) "A Multiscale integrated approach to the study of the nervous system in health and disease" (DN. 1553 11.10.2022) to AR, AB, and GP. Additionally, this study received funding by the Apulia regional government (“Early Identification of Psychosis Risk”) to AB and by the National Institute of Mental Health (RO1 MH094328, “Mismatch Negativity and complex second-order sensory memory in schizophrenia” and R01 MH126951, “Systems-Level Dysconnectivity in First Episode Psychosis”) to DFS.

CRediT authorship contribution statement

Christian Valt: Writing – review & editing, Writing – original draft, Visualization, Methodology, Funding acquisition, Formal analysis, Conceptualization, Investigation, Project administration. **Fran López-Caballero:** Writing – review & editing, Conceptualization, Formal analysis, Investigation, Methodology, Validation, Visualization, Writing – original draft. **Angelantonio Tavella:** Writing – review & editing, Conceptualization, Formal analysis, Investigation. **Mario Altamura:** Writing – review & editing, Resources, Conceptualization. **Antonello Bellomo:** Writing – review & editing, Resources, Conceptualization. **Giuseppe Barrasso:** Writing – review & editing, Resources, Conceptualization. **Brian Coffman:** Writing – review & editing, Methodology, Conceptualization, Formal analysis, Investigation, Project administration, Supervision. **Filippo Iovine:** Writing – review & editing, Resources, Conceptualization. **Antonio Rampino:** Writing – review & editing, Supervision, Conceptualization, Funding acquisition, Resources. **Alessandro Saponaro:** Writing – review & editing, Resources. **Dylan Seebold:** Project administration, Data curation, Investigation, Writing – review & editing. **Pierluigi Selvaggi:** Writing – review & editing, Resources, Conceptualization, Methodology. **Domenico Semisa:** Writing – review & editing, Resources, Conceptualization. **Giuseppe Stolfa:** Project administration, Data curation, Investigation, Writing – review & editing. **Alessandro Bertolino:** Writing – review & editing, Supervision, Resources, Funding acquisition, Conceptualization, Investigation, Methodology. **Giulio Pergola:** Writing – review & editing, Writing – original draft, Supervision, Methodology, Funding acquisition, Conceptualization, Investigation, Project administration, Resources. **Dean F. Salisbury:** Writing – review & editing, Writing – original draft, Supervision, Resources, Methodology, Conceptualization, Funding acquisition, Investigation, Project administration.

Declaration of competing interest

AB has received lecture fees from Otsuka, Janssen, and Lundbeck, as well as consultant fees from Biogen. GP has received lecture fees from Lundbeck. All other authors report no conflicts of interest.

Acknowledgments

We thank Anna Montemurno, Dr. Tiziana Quarto, Dr. Gabriele Russo, Giuseppina Tancredi, Vanessa Fishel, and Natasha Torrence for their help with MEG recording.

Supplementary materials

Supplementary material associated with this article can be found, in the online version, at doi:10.1016/j.psychres.2024.116189.

References

Aeberli, T., Müller, M., Theodoridou, A., Hagenmuller, F., Seifritz, E., Walitza, S., Rössler, W., Kawohl, W., Heekeren, K., 2023. Mismatch Negativity generation in subjects at risk for psychosis: source analysis is more sensitive than surface electrodes in risk prediction. Front. Psychiatry 14, 1130809. https://doi.org/10.3389/fpsyt.2023.1130809.

Baillet, S., Mosher, J.C., Leahy, R.M., 2001. Electromagnetic brain mapping. IEEE Signal Process. Mag. 18 (6), 14–30. https://doi.org/10.1109/79.962275.

Braeutigam, S., Dima, D., Frangou, S., James, A., 2018. Dissociable auditory mismatch response and connectivity patterns in adolescents with schizophrenia and adolescents with bipolar disorder with psychosis: a magnetoencephalography study. Schizophr. Res. 193, 313–318. https://doi.org/10.1016/j.schres.2017.07.048.

Chao, Z.C., Takaura, K., Wang, L., Fujii, N., Dehaene, S., 2018. Large-scale cortical networks for hierarchical prediction and prediction error in the primate brain. Neuron 100 (5), 1252–1266. https://doi.org/10.1016/j.neuron.2018.10.004.

Curtis, M.T., Coffman, B.A., Salisbury, D.F., 2021. Pitch and duration Mismatch Negativity are associated with distinct auditory cortex and inferior frontal cortex volumes in the first-episode schizophrenia spectrum. Schizophr. Bull. Open 2 (1), sgab005. https://doi.org/10.1093/schizbullopen/sgab005.

Dale, A.M., Liu, A.K., Fischl, B.R., Buckner, R.L., Belliveau, J.W., Lewine, J.D., Halgren, E., 2000. Dynamic statistical parametric mapping: combining fMRI and MEG for high-resolution imaging of cortical activity. Neuron 26 (1), 55–67. https://doi.org/10.1016/s0896-6273(00)81138-1.

David, O., Kiebel, S.J., Harrison, L.M., Mattout, J., Kilner, J.M., Friston, K.J., 2006. Dynamic causal modeling of evoked responses in EEG and MEG. Neuroimage 30 (4), 1255–1272. https://doi.org/10.1016/j.neuroimage.2005.10.045.

De Pablo, G.S., Radua, J., Pereira, J., Bonoldi, I., Arienti, V., Besana, F., Soardo, L., Cabras, A., Fortea, L., Catalan, A., Vaquerizo-Serrano, J., Coronelli, F., Kaur, S., Da Silva, J., Shin, J.I., Solmi, M., Brondino, N., Politi, P., McGuire, P., Fusar-Poli, P., 2021. Probability of transition to psychosis in individuals at clinical high risk: an updated meta-analysis. JAMA Psychiatry 78 (9), 970–978. https://doi.org/10.1001/jamapsychiatry.2021.0830.

Destrieux, C., Fischl, B., Dale, A., Halgren, E., 2010. Automatic parcellation of human cortical gyri and sulci using standard anatomical nomenclature. Neuroimage 53 (1), 1–15. https://doi.org/10.1016/j.neuroimage.2010.06.010.

Dheerendra, P., Grent, T., Gajwani, R., Gross, J., Gumley, A.I., Krishnadas, R., Lawrie, S. M., Schwannauer, M., Schultze-Lutter, F., Uhlhaas, P.J., 2024. Intact Mismatch Negativity responses in clinical high risk for psychosis and first-episode psychosis: evidence from source-reconstructed event-related fields and time-frequency data. Biol. Psychiatry Cogn. Neurosci. Neuroimaging 9 (1), 121–131. https://doi.org/10.1016/j.bpsc.2023.09.006.

Dima, D., Frangou, S., Burge, L., Braeutigam, S., James, A.C., 2012. Abnormal intrinsic and extrinsic connectivity within the magnetic Mismatch Negativity brain network in schizophrenia: a preliminary study. Schizophr. Res. 135 (1–3), 23–27. https://doi.org/10.1016/j.schres.2011.12.024.

Erickson, M.A., Ruffle, A., Gold, J.M., 2016. A meta-analysis of Mismatch Negativity in schizophrenia: from clinical risk to disease specificity and progression. Biol. Psychiatry 79 (12), 980–987. https://doi.org/10.1016/j.biopsych.2015.08.025.

First, M.B., Williams, J.B.W., Karg, R.S., Spitzer, R., 2014. Structured clinical interview for DSM-5—Research Version (SCID-5 for DSM-5, Research Version; SCID-5-RV). Encycl. Clin. Psychol. 1–6. https://doi.org/10.1002/9781118625392.wbecp351.

Friston, K.J., 2005. A theory of cortical responses. Philos. Trans. R Soc. Lond. B. Biol. Sci. 360 (1456), 815–836. https://doi.org/10.1098/rstb.2005.1622.

Friston, K.J., Brown, H.R., Siemerkus, J., Stephan, K.E., 2016. The dysconnection hypothesis (2016). Schizophr. Res. 176 (2–3), 83–94. https://doi.org/10.1016/j.schres.2016.07.014.

Friston, K.J., Frith, C.D., 1995. Schizophrenia: a disconnection syndrome. Clin. Neurosci. 3 (2), 89–97.

Friston, K.J., Moran, R., Seth, A.K., 2013. Analysing connectivity with Granger causality and dynamic causal modelling. Curr. Opin. Neurobiol. 23 (2), 172–178. https://doi.org/10.1016/j.conb.2012.11.010.

Fuentemilla, L.L., Marco-Pallarés, J., Münte, T.F., Grau, C., 2008. Theta EEG oscillatory activity and auditory change detection. Brain Res. 1220, 93–101. https://doi.org/10.1016/j.brainres.2007.07.079.

Garrido, M.I., Kilner, J.M., Kiebel, S.J., Friston, K.J., 2007. Evoked brain responses are generated by feedback loops. Proc. Natl. Acad. Sci. U. S. A. 104 (52), 20961–20966. https://doi.org/10.1073/pnas.0706274105.

Garrido, M.I., Kilner, J.M., Stephan, K.E., Friston, K.J., 2009. The Mismatch Negativity: a review of underlying mechanisms. Clin. Neurophysiol. 120 (3), 453–463. https://doi.org/10.1016/j.clinph.2008.11.029.

Gaser, C., Dahnke, R., Thompson, P.M., Kurth, F., Luders, E., Alzheimer’s Disease Neuroimaging Initiative, 2024. CAT–A computational anatomy toolbox for the analysis of structural MRI data. GigaScience 13, 1–13. 10.1093/gigascience/giae049.

Haenschel, C., Baldeweg, T., Croft, R.J., Whittington, M., Gruzelier, J., 2000. Gamma and beta frequency oscillations in response to novel auditory stimuli: a comparison of human electroencephalogram (EEG) data with *in vitro* models. Proc. Natl. Acad. Sci. U. S. A. 97 (13), 7645–7650. https://doi.org/10.1073/pnas.120162397.

Hamilton, H.K., Roach, B.J., Bachman, P.M., Belger, A., Carrión, R.E., Duncan, E., Johannesen, J.K., Light, G.A., Niznikiewicz, M.A., Addington, J., Bearden, C.E., Cadenhead, K.S., Cornblatt, B.A., McGlashan, T.H., Perkins, D.O., Tsuang, M.T., Walker, E.F., Woods, S.W., Cannon, T.D., Mathalon, D.H., 2022. Mismatch Negativity in response to auditory deviance and risk for future psychosis in youth at clinical high risk for psychosis. JAMA Psychiatry 79 (8), 780–789. https://doi.org/10.1001/jamapsychiatry.2022.1417.

Javitt, D.C., Lee, M., Kantrowitz, J.T., Martinez, A., 2018. Mismatch Negativity as a biomarker of theta band oscillatory dysfunction in schizophrenia. Schizophr. Res. 191, 51–60. https://doi.org/10.1016/j.schres.2017.06.023.

Kim, S., Baek, J.H., Shim, S.H., Kwon, Y.J., Lee, H.Y., Yoo, J.H., Kim, J.S., 2020. Mismatch Negativity indices and functional outcomes in unipolar and bipolar depression. Sci. Rep. 10 (1), 12831. https://doi.org/10.1038/s41598-020-69776-4.

Kirihara, K., Tada, M., Koshiyama, D., Fujioka, M., Usui, K., Araki, T., Kasai, K., 2020. A predictive coding perspective on Mismatch Negativity impairment in schizophrenia. Front. Psychiatry 11, 660. https://doi.org/10.3389/fpsyt.2020.00660.

Kool, L., Oranje, B., Meijs, H., De Wilde, B., Van Hecke, J., Niemegeers, P., Luykx, J.J., 2022. Event-related potentials and use of psychotropic medication in major psychiatric disorders. Psychiatry Res. 314, 114637. https://doi.org/10.1016/j.psychres.2022.114637.

Koshiyama, D., Miyakoshi, M., Joshi, Y.B., Molina, J.L., Tanaka-Koshiyama, K., Sprock, J., Braff, D.L., Swerdlow, N.R., Light, G.A., 2020. Abnormal effective connectivity underlying auditory Mismatch Negativity impairments in schizophrenia. Biol. Psychiatry Cogn. Neurosci. Neuroimaging 5 (11), 1028–1039. https://doi.org/10.1016/j.bpsc.2020.05.011.

Lakatos, P., O'Connell, M.N., Barczak, A., McGinnis, T., Neymotin, S., Schroeder, C.E., Smiley, J.F., Javitt, D.C., 2020. The thalamocortical circuit of auditory Mismatch Negativity. Biol. Psychiatry 87 (8), 770–780. https://doi.org/10.1016/j.biopsych.2019.10.029.

Larsen, K.M., Dzafic, I., Darke, H., Pertile, H., Carter, O., Sundram, S., Garrido, M.I., 2020. Aberrant connectivity in auditory precision encoding in schizophrenia spectrum disorder and across the continuum of psychotic-like experiences. Schizophr. Res. 222, 185–194. https://doi.org/10.1016/j.schres.2020.05.061.

Lee, M., Sehatpour, P., Hoptman, M.J., Lakatos, P., Dias, E.C., Kantrowitz, J.T., Martinez, A.M., Javitt, D.C., 2017. Neural mechanisms of Mismatch Negativity dysfunction in schizophrenia. Mol. Psychiatry 22 (11), 1585–1593. https://doi.org/10.1038/mp.2017.3.

Li, X., Deng, W., Xue, R., Wang, Q., Ren, H., Wei, W., Zhang, Y., Li, M., Zhao, L., Du, X., Meng, Y., Ma, X., Hall, M.H., Li, T., 2023. Auditory event-related potentials, neurocognition, and global functioning in drug naïve first-episode schizophrenia and bipolar disorder. Psychol. Med. 53 (3), 785–794. https://doi.org/10.1017/S0033291721002130.

Lieder, F., Stephan, K.E., Daunizeau, J., Garrido, M.I., Friston, K.J., 2013. A neurocomputational model of the Mismatch Negativity. PLoS Comput. Biol. 9 (11), e1003288. https://doi.org/10.1371/journal.pcbi.1003288.

López-Caballero, F., Auksztulewicz, R., Howard, Z., Rosch, R.E., Todd, J., Salisbury, D.F., 2024. Computational synaptic modeling of pitch and duration Mismatch Negativity in first-episode psychosis reveals selective dysfunction of the N-methyl-D-Aspartate (NMDA) receptor. Clin. EEG Neurosci. https://doi.org/10.1177/15500594241238294.

López-Caballero, F., Curtis, M., Coffman, B.A., Salisbury, D.F., 2023. Is source-resolved magnetoencephalographic Mismatch Negativity a viable biomarker for early psychosis? Eur. J. Neurosci. https://doi.org/10.1111/ejn.16432.

Michie, P.T., Budd, T.W., Todd, J., Rock, D., Wichmann, H., Box, J., Jablensky, A.V., 2000. Duration and frequency Mismatch Negativity in schizophrenia. Clin. Neurophysiol. 111 (6), 1054–1065. https://doi.org/10.1016/s1388-2457(00)00275-3.

Näätänen, R., Kähkönen, S., 2009. Central auditory dysfunction in schizophrenia as revealed by the Mismatch Negativity (MMN) and its magnetic equivalent MMNm: a review. Int. J. Neuropsychopharmacol. 12 (1), 125–135. https://doi.org/10.1017/S1461145708009322.

Näätänen, R., Kujala, T., Winkler, I., 2011. Auditory processing that leads to conscious perception: a unique window to central auditory processing opened by the Mismatch Negativity and related responses. Psychophysiology 48 (1), 4–22. https://doi.org/10.1111/j.1469-8986.2010.01114.x.

Näätänen, R., Paavilainen, P., Rinne, T., Alho, K., 2007. The Mismatch Negativity (MMN) in basic research of central auditory processing: a review. Clin. Neurophysiol. 118 (12), 2544–2590. https://doi.org/10.1016/j.clinph.2007.04.026.

Näätänen, R., Todd, J., Schall, U., 2016. Mismatch Negativity (MMN) as biomarker predicting psychosis in clinically at-risk individuals. Biol. Psychol. 116, 36–40. https://doi.org/10.1016/j.biopsycho.2015.10.010.

Nicol, R.M., Chapman, S.C., Vértes, P.E., Nathan, P.J., Smith, M.L., Shtyrov, Y., Bullmore, E.T., 2012. Fast reconfiguration of high-frequency brain networks in response to surprising changes in auditory input. J. Neurophysiol. 107 (5), 1421–1430. https://doi.org/10.1152/jn.00817.2011.

Recasens, M., Gross, J., Uhlhaas, P.J., 2018. Low-frequency oscillatory correlates of auditory predictive processing in cortical-subcortical networks: a MEG-study. Sci. Rep. 8 (1), 14007. https://doi.org/10.1038/s41598-018-32385-3.

Salisbury, D.F., Kuroki, N., Kasai, K., Shenton, M.E., McCarley, R.W., 2007. Progressive and interrelated functional and structural evidence of post-onset brain reduction in schizophrenia. Arch. Gen. Psychiatry 64 (5), 521–529. https://doi.org/10.1001/archpsyc.64.5.521.

Salisbury, D.F., Shafer, A.R., Murphy, T.K., Haigh, S.M., Coffman, B.A., 2020. Pitch and duration Mismatch Negativity and Heschl's gyrus volume in first-episode schizophrenia-spectrum individuals. Clin. EEG Neurosci. 51 (6), 359–364. https://doi.org/10.1177/1550059420914214.

Salisbury, D.F., Shenton, M.E., Griggs, C.B., Bonner-Jackson, A., McCarley, R.W., 2002. Mismatch Negativity in chronic schizophrenia and first-episode schizophrenia. Arch. Gen. Psychiatry 59 (8), 686–694. https://doi.org/10.1001/archpsyc.59.8.686.

Sauer, A., Grent, T., Zeev-Wolf, M., Singer, W., Goldstein, A., Uhlhaas, P.J., 2023. Spectral and phase-coherence correlates of impaired auditory Mismatch Negativity (MMN) in schizophrenia: a MEG study. Schizophr. Res. 261, 60–71. https://doi.org/10.1016/j.schres.2023.08.033.

Schofield, T.M., Iverson, P., Kiebel, S.J., Stephan, K.E., Kilner, J.M., Friston, K.J., Crinion, J.T., Price, C.J., Leff, A.P., 2009. Changing meaning causes coupling changes within higher levels of the cortical hierarchy. Proc. Natl. Acad. Sci. U. S. A. 106 (28), 11765–11770. https://doi.org/10.1073/pnas.0811402106.

Suda, Y., Tada, M., Matsuo, T., Kawasaki, K., Saigusa, T., Ishida, M., Mitsui, T., Kumano, H., Kirihara, K., Suzuki, T., Matsumoto, K., Hasegawa, I., Kasai, K., Uka, T., 2022. Prediction-related frontal-temporal network for omission mismatch activity in the macaque monkey. Front. Psychiatry 13, 557954. https://doi.org/10.3389/fpsyt.2022.557954.

Tada, M., Kirihara, K., Mizutani, S., Uka, T., Kunii, N., Koshiyama, D., Fujioka, M., Usui, K., Nagai, T., Araki, T., Kasai, K., 2019. Mismatch Negativity (MMN) as a tool for translational investigations into early psychosis: a review. Int. J. Psychophysiol. 145, 5–14. https://doi.org/10.1016/j.ijpsycho.2019.02.009.

Tadel, F., Baillet, S., Mosher, J.C., Pantazis, D., Leahy, R.M., 2011. Brainstorm: a user-friendly application for MEG/EEG analysis. Comput. Intell. Neurosci. 2011, 1–13. https://doi.org/10.1155/2011/879716.

Tadel, F., Bock, E., Niso, G., Mosher, J.C., Cousineau, M., Pantazis, D., Leahy, R.M., Baillet, S., 2019. MEG/EEG group analysis with brainstorm. Front. Neurosci. 76. https://doi.org/10.3389/fnins.2019.00076.

Taulu, S., Simola, J., 2006. Spatiotemporal signal space separation method for rejecting nearby interference in MEG measurements. Phys. Med. Biol. 51 (7), 1759. https://doi.org/10.1088/0031-9155/51/7/008.

Todd, J., Howard, Z., Auksztulewicz, R., Salisbury, D.F., 2023a. Computational modeling of oddball sequence processing exposes common and differential auditory network changes in first-episode schizophrenia-spectrum disorders and schizophrenia. Schizophr. Bull. 49 (2), 407–416. https://doi.org/10.1093/schbul/sbac153.

Todd, J., Salisbury, D., Michie, P.T., 2023b. Why Mismatch Negativity continues to hold potential in probing altered brain function in schizophrenia. Psychiatry Clin. Neurosci. Rep. 2 (3), e144. https://doi.org/10.1002/pcn5.144.

Tseng, Y.J., Nouchi, R., Cheng, C.H., 2021. Mismatch Negativity in patients with major depressive disorder: a meta-analysis. Clin. Neurophysiol. 132 (10), 2654–2665. https://doi.org/10.1016/j.clinph.2021.06.019.

Umbricht, D., Koller, R., Schmid, L., Skrabo, A., Grübel, C., Huber, T., Stassen, H., 2003. How specific are deficits in Mismatch Negativity generation to schizophrenia? Biol. Psychiatry 53 (12), 1120–1131. https://doi.org/10.1016/s0006-3223(02)01642-6.

Valt, C., Quarto, T., Tavella, A., Romanelli, F., Fazio, L., Arcara, G., Altamura, M., Barrasso, G., Bellomo, A., Blasi, G., Brudaglio, F., Carofiglio, A., D'Ambrosio, E., Padalino, F.A., Rampino, A., Saponaro, A., Semisa, D., Suma, D., Pergola, G., Bertolino, A., 2023. Reduced magnetic Mismatch Negativity: a shared deficit in psychosis and related risk. Psychol. Med. 53 (13), 6037–6045. https://doi.org/10.1017/S003329172200321X.

Wang, B., Zartaloudi, E., Linden, J.F., Bramon, E., 2022. Neurophysiology in psychosis: the quest for disease biomarkers. Transl. Psychiatry 12 (1), 100. https://doi.org/10.1038/s41398-022-01860-x.

Xia, C., Li, J., Yan, R., Su, W., Liu, Y., 2023. Contribution of inter-trial phase coherence at theta, alpha, and beta frequencies in auditory change detection. Front. Neurosci. 17. https://doi.org/10.3389/fnins.2023.1224479.

Yüksel, M., Murphy, M., Rippe, J., Leicht, G., Öngür, D., 2021. Decreased Mismatch Negativity and elevated frontal-lateral connectivity in first-episode psychosis. J. Psychiatr. Res. 144, 37–44. https://doi.org/10.1016/j.jpsychires.2021.09.034.

Yung, A.R., Yung, A.R., Pan Yuen, H., Mcgorry, P.D., Phillips, L.J., Kelly, D., Dell'olio, M., Francey, S.M., Cosgrave, E.M., Killackey, E., Stanford, C., Godfrey, K., Buckby, J., 2005. Mapping the onset of psychosis: the comprehensive assessment of at-risk mental states. Aust. N. Z. J. Psychiatry 39 (11–12), 964–971. https://doi.org/10.1080/j.1440-1614.2005.01714.x.